Nano Scale Disruptive Silicon-Plasmonic Platform for Chip-to-Chip Interconnection

Demonstration of conductive QD layers with photoconductive properties

Milestone no.:	MS.18
Due date:	01/31/2013
Actual Submission date:	01/31/2013
Authors:	UVEG
Work package(s):	WP4
Distribution level:	RE[1] (NAVOLCHI Consortium)
Nature:	document, available online in the restricted area of the NAVOLCHI webpage

List of Partners concerned

Partner number	Partner name	Partner short name	Country	Date enter project	Date exit project
5	UNIVERSITAT DE VALENCIA	UVEG	Spain	M1	M36

[1] **PU** = Public
PP = Restricted to other programme participants (including the Commission Services)
RE = Restricted to a group specified by the consortium (including the Commission Services)
CO = Confidential, only for members of the consortium (including the Commission Services)

Deliverable Responsible

Organization: University of Valencia Estudi General (UVEG)
Contact Person: Juan P. Martínez Pastor
Address: Instituto de Ciencia de los Materiales, Universidad de Valencia
P.O. Box 22085
46071 Valencia
Spain
Phone: +34 963544793
Fax: +34 963543633
E-mail: martinep@uv.es

Executive Summary

This document shall incorporate (all) rules procedures concerning the technical and administrative management of the project and is therefore to be updated on a regular basis. Please look at www.navolchi.eu regularly for the latest version.

Change Records

Version	Date	Changes	Author
1	2013-01-14		Pedro Rodríguez Cantó
2	2013-01-30		Juan P. Martínez Pastor
3	2013-01-31		Pedro Rodríguez Cantó
4	2013-01-31		Juan P. Martínez Pastor
5	2013-02-02		Pedro Rodríguez Cantó
6	2013-02-03		Juan P. Martínez Pastor

1. Introduction

A signal generated at the plasmonic transmitter chip (laser plus modulator) has to be measured by a plasmonic receiver in order to be processed electronically. For this purpose, the receiver needs to accomplish the following conditions. Firstly, low-level signals coupled to a plasmonic waveguide (photons are transformed into propagating Surface Plasmon Polaritons -SPPs-) will be amplified before the input of the detector in order to enhance the sensitivity of the receiver. Secondly, the incoming signal in the detector will convert the amplified SPPs into an electrical signal. With the intention to improve the chip-to-chip interconnection integration, amplifier and detector will be designed into the same silicon substrate, as it is illustrated in figure 1.

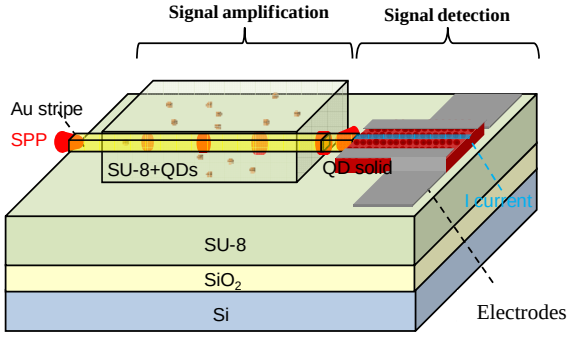

Figure 1. Plasmonic receiver composed by a SPP amplifier and a photodetector.

The photodetector will consist in a conductive layer of PbS (or PbSe) quantum dots (QDs), whose thickness should be optimized, able to generate an electrical current as a response of the incoming photons [1]. Reported responsivities in recent literature are in the range of 0.1-3.9 A/W for a PbS QD monolayer in a nanogap photoconductor [2], larger than 100 A/W for a PbS layer thicker than 200 nm [3] and more than 10^6 A/W in a MOS structure based on a PbS layer (60-80 nm thick) on graphene [4]. The QD-solid approximation is considered one of the latest advanced concepts for photodetection, given the high absorption of quantum dots, the low cost of the solution processing technique used to deposit the material as well as its integration in Si technology. Furthermore, this concept can be easily combined with plasmonic layers based on metal nanoparticles, because an enhancement of the responsivity is expected due to light trapping effect at the band edge of the QD-solid [3].

To achieve the goals proposed in this project, we have accomplished following outcomes so far:

- Synthesis and characterization of infrared colloidal QDs (PbS and PbSe).
- Preparation and characterization of QD-solids based on these nanoestructures.
- Electrical Characterization of the fabricated devices.

2. Synthesis of "infrared" QDs

Synthesis of PbS QDs

The synthesis of QDs for IR is based on the hot injection of metal-organic precursors into coordinating/non-coordinating solvents at elevated temperatures. This strategy is established to be the mainstream strategy in the synthesis of high quality semiconductor nanocrystals. Thus, we carried out the synthesis of PbS QDs using lead oleate and bis(trimethylsilyl) sulfide (TMS) as precursors. We use a Pb to S precursor ratio set as 2:1, within the typical range employed in cadmium chalcogenide and lead chalcogenide nanocrystal synthesis [5]. We employed slow cooling following sulfur precursor injection to facilitate size focusing in the hope of achieving a narrow size distribution and well-defined excitonic structure.

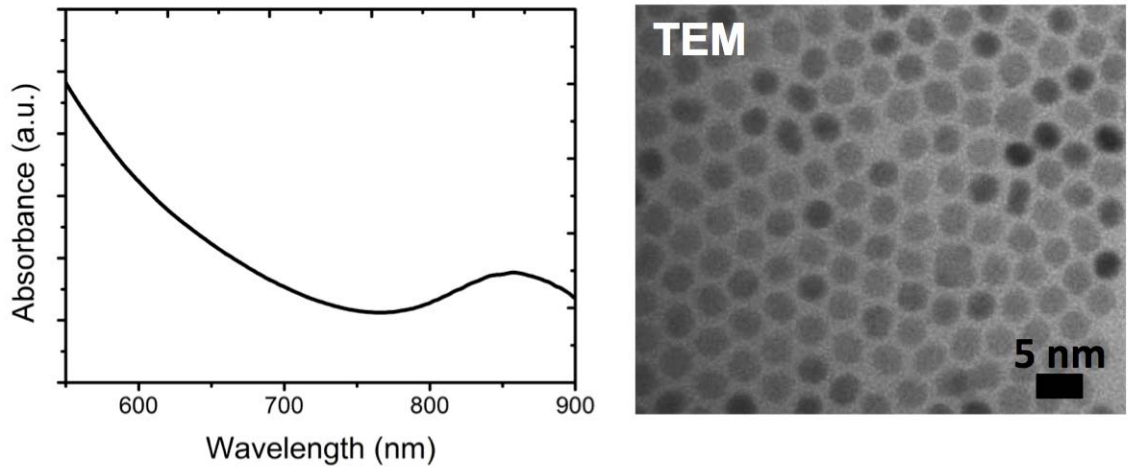

Figure 2: Absorption spectrum of as-synthesized PbS colloidal QDs in toluene (left) and TEM image of these PbS QDs.

Figure 2 shows the absorbance spectrum of acid oleic-capped PbS colloidal QDs in toluene. As can be observed PbS QDs showed a well-defined excitonic peak centred at around 870 nm. The average size of them was 3.2 nm (Fig. 2 right), approximately, as calculated from the equation proposed by Iwan Moreels *et al.* [6]:

$$E^0 = 0.41 + (0.0252d^2 + 0.283d)^{-1}$$

where E_0 is the effective bandgap (1.30 eV in the case of QDs in Fig. 2) and d is the PbS QD diameter in nm.

Before the fabrication of QDs films, we purified the colloidal QDs by selective precipitation using non-solvents (acetone/methanol mixture). We carried out a ligand exchange reaction by dispersing oleate-capped PbS in oleylamine, which has the same molecular size as oleic acid but exhibits less affinity to PbS. Therefore, the bond between PbS and oleylamine is weaker than oleate, which is necessary for the creation of the QD solid, as describe below. After this partial ligand exchange, absorption is blue-shifted 10 nm. QDs are purified again by selective precipitation with methanol and then redispersed in octane at a concentration of 20 mg/mL, typically.

Synthesis of PbSe QDs

Similar to the synthesis of PbS QDs, we have also optimized the production of monodisperse PbSe QDs with different sizes having their excitonic peak in the range 1300-1900 nm, as shown in Fig. 3. They were synthesized following the procedure reported in [7].

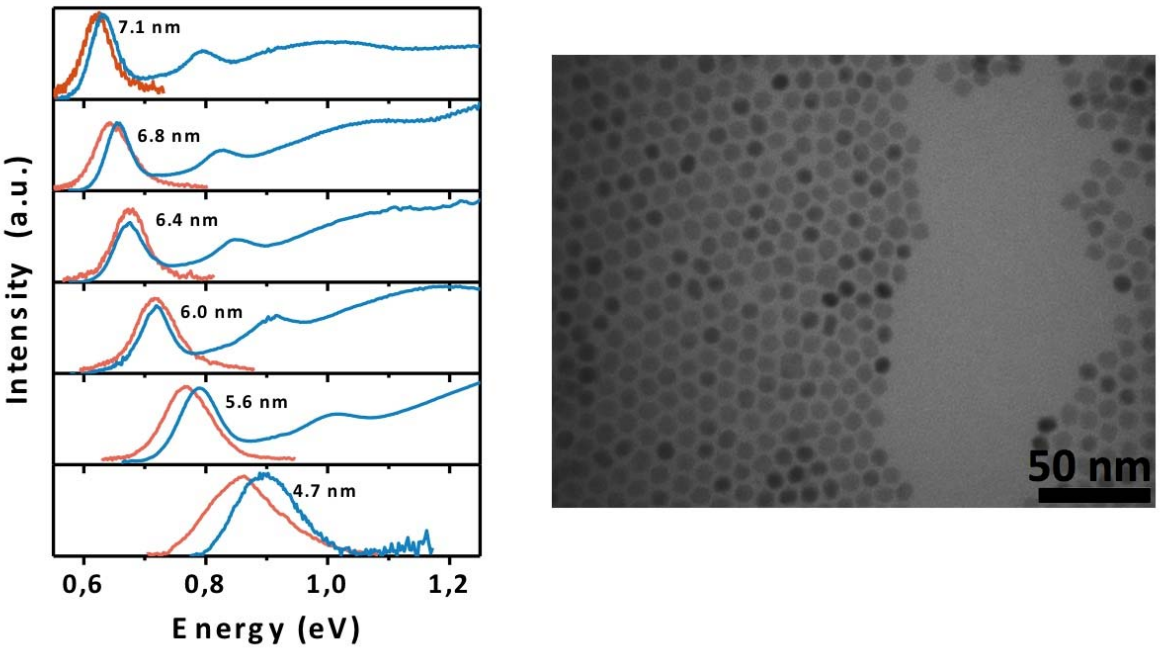

Figure 3: Absorption and PL spectra of colloidal PbSe QDs with different sizes ranging from 4.7 to 7.1 nm (left). TEM image of PbSe QDs with an average size of about 7 nm (right).

3. Preparation and characterization of QD-solids

The production of QD-solids is based on a solution-processing method called Layer-by-Layer (LbL), which is illustrated in Fig. 4. This approach allows the fabrication of smooth and crevice-free QD films directly from the colloidal solution. In a first step, we used spherical PbS QDs for the fabrication of layer stacks and carried out their basic characterization. The key step of this method consists in a ligand exchange reaction to replace the insulating oleyamine (2 nm long) for shorter ligands. The new ligand used is bidentate in order to closely interconnect QDs. In the measure that the distance between nanocrystals is reduced, the electron and hole transport is significantly improved. It is important to note that the end functional group itself plays an important role in the passivation of the nanocrystal surface and thus the control of midgap states and shallow traps.
Typically, PbS QD films were deposited on glass or glass/ITO substrates through the LbL spin-coating process. Each layer deposition consisted of four deposition steps during spinning by dropping: 1) PbS solution in octane; 2) 1% bidentate ligand solution (ethanedithiol (EDT), 3-Mercaptopropionic acid (MPA), oxalic acid, …); 3) anhydrous acetonitrile (or methanol in case of MPA); 4) anhydrous octane. We repeat these steps 4-10 times to obtain smooth quantum dot films 200-300 nm thick, as measured by a mechanical profilometer.

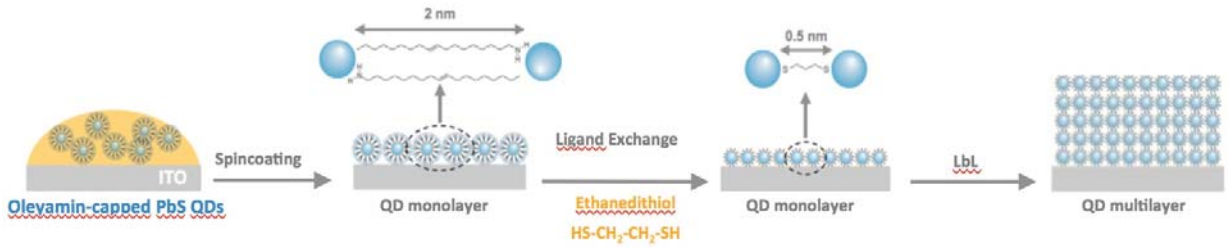

Figure 4. Scheme of the LBL approach.

The optical properties were preserved after ligand exchange, as shown in Fig. 5. TEM images in Fig. 6 show a monolayer before and after the ligand exchange procedure, where the reduction of the average QD interdistance is clearly observed (i.e., the original oleylamine ligands are completely exchanged by the shorter ligands).

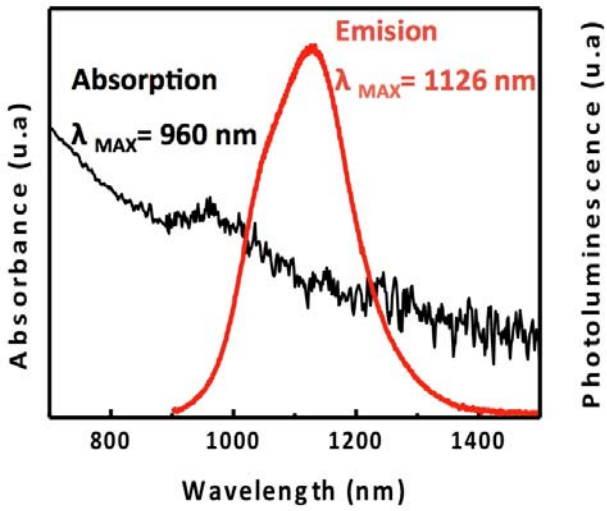

Figure 5: Absorption and PL spectra of EDT-capped PbS film.

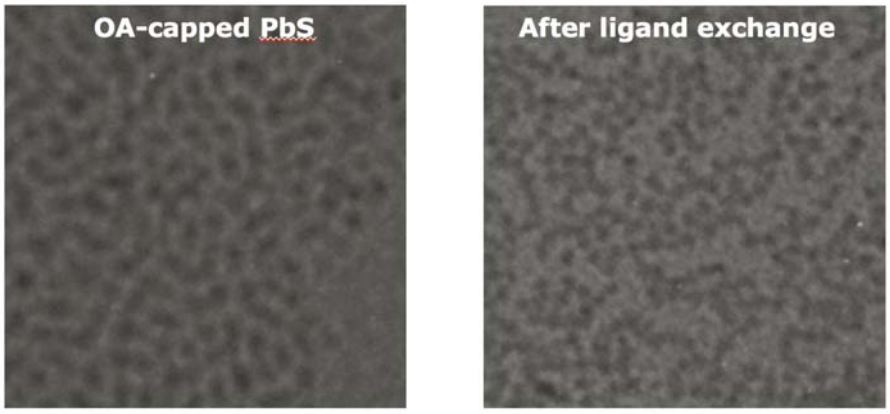

Figure 6. TEM images of a PbS monolayer before and after ligand exchange.

In order to evaluate the surface chemistry of the PbS NCs in the fabricated films we used XPS measurements (Fig. 7). We focused on the S 2p XPS peak to analyze the oxidation species and followed the Pb 4d peak only as a consistency check. Detailed spectral deconvolution of both S 2p and Pb 4d high resolution XPS spectra allows us to distinguish the sulphur-containing oxidation products polythiol S-S, lead sulphite ($PbSO_3$), and lead sulphate ($PbSO_4$).

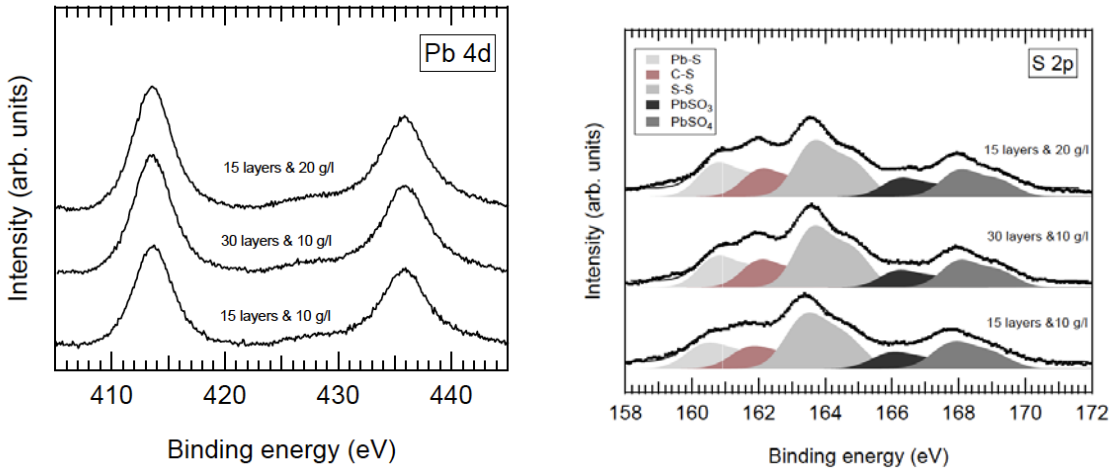

Figure 7. XPS data obtained for LBL-produced films of PbS NCs using EDT for ligand exchange.

Among the bidentate ligands tested for the fabrication of layer stacks, we decided to start investigating MPA instead of EDT, thioglicolic acid or oxalic acid. Ligand passivation strongly influences the charge carrier mobility, as well as recombination properties in this type of films. As reported in [8], MPA passivation may enable significant enhancement of the carrier mobility-lifetime product in the PbS QD solid leading to an increase in both the diffusion length of charge carriers and the photon conversion efficiencies. The origin of such enhancement is due to a lower density and energetic distribution of charge traps in MPA-processed PbS QD films. Simultaneously, the lower density of charge traps decreases the bimolecular charge recombination rate in comparison to the rate expected from the increase in carrier mobility. MPA provides greater chemical diversity in comparison to EDT (presenting both thiol and carboxylate functional groups to PbS surfaces) and is therefore able to passivize a broader distribution of surface states.

4. Photocurrent in QD-solids

Previous studies in literature developed on PbS photoconductors have shown that photosensitization of PbS is followed by oxidation, and in particular formation of lead sulphates ($PbSO_4$). They act as sensitizing centres that prolong the minority (electron) carrier lifetime allowing holes to transverse the device within this carrier lifetime. We maintain this hypothesis, but further studies will be developed to determine the generation/recombination mechanism in our material. For the moment, we have established a technological processing, as described above, for a reproducible preparation of QD solids. These layers and devices maintain their good electro-optical properties stable during weeks in air. They exhibit photoconductive properties as shown below, even if still we continue to work actively on the chemistry to improve the optical quality of the IV-VI QDs. This is necessary for understanding the physics of the device and introducing surface traps for electrons in a controlled way, if necessary.

In the last months we have mounted an in-house set-up to measure the spectral photoconductivy/photocurrent/photovoltage based on la Xe-lamp (150 W), monochromator 300 mm of focal length, low-noise pre-amplifier and lock-in electronics and a calibrated Si-photodiode to obtain responsivity values. In parallel we also use a Keithley 2400 source-meter for measuring I(V) characteristics under dark or illumination conditions (monochromatic light or the whole lamp spectrum). Then, we are able to measure weak and intermediate/large photocurrent signals by using the first and second type of measurements, respectively.
We have deposited lateral electrodes on top of the QD film deposited on glass, but photocurrent was very low given the large distance between electrodes with our available mask (100 μm, which leads to very weak electric fields, in the order of 10 mV/μm for 1 V). We are defining at the moment a mask to produce patterns by UV photolithography for the deposition of electrodes separated in the range of 2 to 10 μm (next generation of devices). Alternative devices consisted in the deposition of the QD film by the LbL method on top of a glass-ITO-PEDOT substrate (front side of the device for incoming light) and covered by silver electrodes (around 4 mm^2 in size). In this way we are obtaining a near-ohmic device with R ≈ 100 Ω (ρ ≈ 2.10^5 Ω cm, which is similar to values obtained by other authors), even if we estimate an internal built-in voltage of the order of 1 mV. In fact, this small internal field is enough to obtain responsivities above 1 mA/W in the visible and 0.2 mA/W in the region where the ground exciton absorption takes place, as shown in Fig. 8. The photocurrent spectrum (measured in the region limits of our calibrated Si-photodetector) is well correlated with the absorbance, except in the region of the first excited state absorption (750-950 nm), where photocurrent exhibit a well pronounced dip. This could be temptatively attributed to some efficient transfer of majority carriers towards defects.

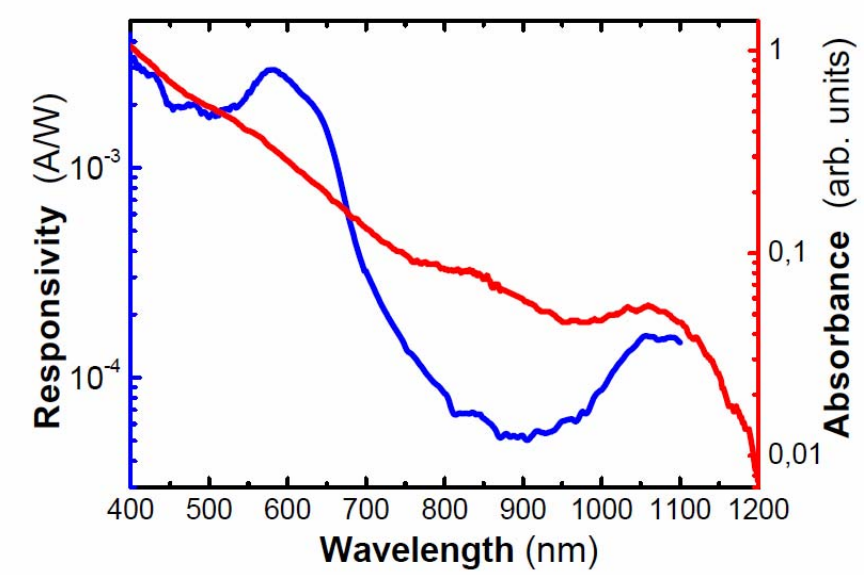

Figure 8. Photocurrent (blue line) compared to absorbance (red line) spectrum measured in a glass/ITO/PEDOT/QD-film/Ag device.

If we measure the photocurrent as the difference between the I(V) curves under illumination (3 mW of white light, approximately) and dark conditions we observe a linear behavior with applied voltage (Fig. 9). The slope of this variation is around 34 μA/V, which can be traduced in a responsivity slightly larger (≈ 10 mA/W) to that estimated by measuring the short circuit photocurrent in the device (Fig. 8). Of course, greater electric fields should be applied without

generating big dark currents (damaging the device) to obtain higher photoconductive gains. This will be possible in new device generations.

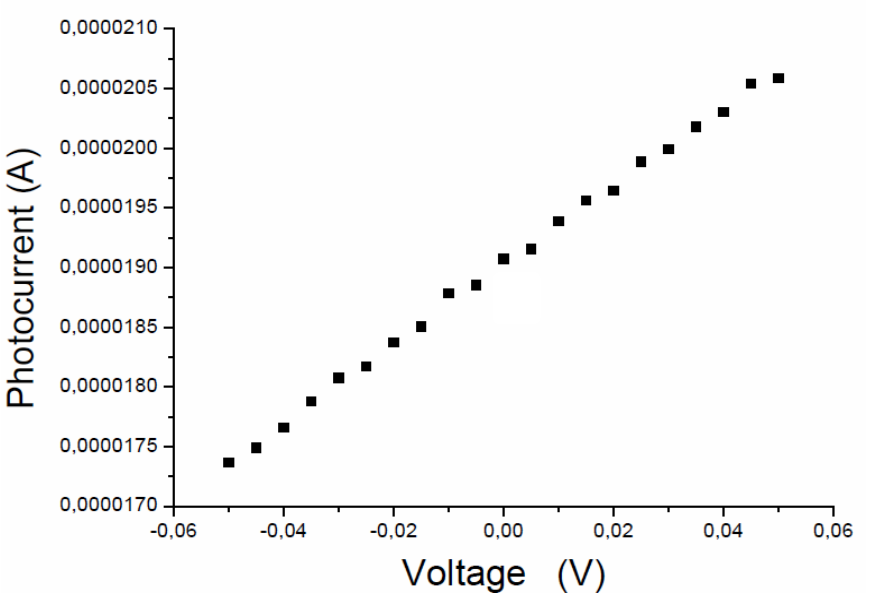

Figure 8. Photocurrent (blue line) compared to absorbance (red line) spectrum measured in a glass/ITO/PEDOT/QD-film/Ag device.

5. Conclusions

PbS and PbSe QDs are synthesized with appropriate diameters to obtain ground exciton absorption in the near infrared (1000 – 1900 nm). QD solids based on PbS have been prepared in a reproducible way, exhibiting oxides at the QD surface and stable in air, as the photodevices fabricated with them. They exhibit appropriate photo-electrical properties for using them in photodetector devices. Next generation of devices will be focused on lateral electrodes separated in the μm-range and PbS (or PbSe) of appropriate size to have absorption at 1550 nm.

References

[1] G. Konstantatos and E.H. Sargent, "Nanostructured materials for photodetection" Nature Nanotechnology, 5, 391-400, 2010.
[2] Ferry Prins, *et al.*: "Fast and Efficient Photodetection in Nanoscale Quantum-Dot Junctions", *Nanolett.*, vol. 12. pp. 5740–5743, October 2012.
[3] F. Pelayo García de Arquer, *et al.*: "Plasmonic light trapping leads to responsivity increase in colloidal quantum dot photodetectors", *Appl. Phys. Lett.*, vol. 100. pp. 043101, Jan. 2012.
[4] G. Konstantatos, *et al.*: "Hybrid graphene–quantum dot phototransistors with ultrahigh gain", *Nat. Nanotech.*, vol. 7. pp. 363-3
[5] Murphy, J. E.; Beard, M. C.; Norman, A. G.; Ahrenkiel, S. P.; Johnson, J. C.; Yu, P. R.; Micic, O. I.; Ellingson, R. J.; Nozik, A. J. J. Am.Chem. Soc. 2006, 128, 3241–3247.
[6] Moreels, I.; Lambert, K.; Smeets, D.; Muynck, D. D.; Nollet, T.; Martins, J. C.; Vanhaecke, F.; Vantomme, A.; Delerue, C.; Allan, G.; Hens, Z. ACS Nano 3, pp. 3023–3030 (2009)
[7] Hui Du, Chialing Chen, Rishikesh Krishnan, Todd D. Krauss, Jeffrey M. Harbold, Frank W. Wise, Malcolm G. Thomas, and John Silcox, "Optical properties of colloidal PbSe nanocrystals," Nanoletters 2 (11, pp. 1321-1324 (2002).
[8] Kwang S. Jeong, Jiang Tang, Huan Liu, *et al.*, Enhanced Mobility-Lifetime Products in PbS Colloidal Quantum Dot Photovoltaics," ACS Nano 6 (1), pp. 89-99 (2012).